Manuscript

Local stress control to suppress dislocation generation for pseudomorphically grown AlGaN UV-C laser diodes

Maki Kushimoto,[1, a)] Ziyi Zhang,[2, 3] Akira Yoshikawa,[2, 3] Koji Aoto,[2, 3] Yoshio Honda,[3] Chiaki Sasaoka,[3] Leo J. Schowalter,[3] and Hiroshi Amano[3]

[1)] *Graduate School of Engineering, Nagoya University, Chikusa, Nagoya, Aichi 464-8603, Japan*

[2)] *Innovative Devices R&D Center, Corporate Research & Development, Asahi Kasei Corporation, Chiyoda, Tokyo 100-0006, Japan*

[3)] *Center for Integrated Research of Future Electronics, Institute of Materials Research and System for Sustainability, Nagoya University, Chikusa, Nagoya, Aichi 464-8601, Japan*

(Dated: 27 October 2022)

Previously reported UV-C laser diodes (LD) structures have been subject to design constraints owing to dark line defects at the edge of the mesa stripe after device fabrication. To address this issue, a detailed analysis revealed that the dark line defects were dislocations generated by local residual shear stresses associated with mesa formation on highly strained epitaxial layers. A technique for controlling the local concentration of shear stress, using a sloped mesa geometry, was proposed based on the insights gained by modeling the stress distribution at the edge of the mesa stripe. Experimental results showed that this technique succeeded in completely suppressing the emergence of dark-line defects. This technique will be useful in improving the performance of pseudomorphic AlGaN/AlN-based optoelectronic device including UV-C LDs.

Laser diodes (LDs), which have an emission wavelength between 270 and 280 nm (in the UV-C range) and which are based on the pseudomorphic growth of AlGaN on AlN substrates, have been demonstrated in prior works[1,2]. However, many practical applications of these devices will require improved performances, including higher efficiency, and better lifetime and reliability. One key issue noted in the prior work was the appearance of dark line defects at the laser strip mesa edges during thermal annealing[3]. The dark line defects deteriorate the active area at the edge of the mesa, forcing the p-electrode to be placed away from the mesa edge so that the current path avoids this area. This limitation of p-electrode placement has been a serious obstacle in reducing the series resistance of UVC-LD devices since it is strongly impacted by the current path length in the n-cladding layer. For instance, continuous-wave (CW) operation of a UV-C LD was recently achieved[2] at 5 °C where the n-AlGaN layer (with 75% Al content) had a resistivity of 0.011 Ω·cm and a thickness of 350 nm. The dark line defects near the edge of the mesa forced the p-electrode to be placed 15 μm from the corner of the mesa trench. For these parameters, in a 600-μm-long laser diode, every 5 μm of extra distance increases the resistance between an n- and p-electrode by 2.6 Ω. Room temperature CW operation could not be achieved because Joule heating from the diode's series resistance increased the junction temperature, which in turn significantly increased the threshold current needed for lasing. Reducing the series resistance by increasing the thickness of the n-cladding layer or decreasing the Al content are severely constrained by the overall thickness limitations required by pseudomorphic growth,[4] which is desired for low defect density,[1,5] and the optimization of electron injection into the waveguide and active layer while achieving sufficient optical confinement[2,6].

[a)] Electronic mail: kushimoto@nuee.nagoya-u.ac.jp

The origin of the dark line defects appeared to be dislocations originating from the mesa edge. Dislocation formation due to the presence of mesas has been reported in other material systems. In those studies, the localized shear stress generated by a strongly strained hetero-interface is mentioned as a driving force for the formation and propagation of dislocations.[7–9] While uniform pseudomorphic AlGaN layers will have uniform compressive strain across the entire wafer (with the exception of the wafer edges), etching mesas into the highly strained layers (for example, a pseudomorphic layer of $Al_xGa_{1-x}N$ with $x = 0.7$ has a compressive strain of 0.7%) produces similar, large localized shear stresses at the mesa corners since the mesa sidewalls are no longer constrained to fit the underlying substrate.[10,11]

In this work, a detailed observation of the regions where dark line defects appeared revealed the contribution of dislocations from the mesa edge. Further analysis was also carried out to understand the nature of these dislocations. The origin of dislocations and the localization of shear stresses are discussed by modeling the stress distribution at the mesa edge using the elastic properties of AlGaN alloys. A practical method to control the local shear stress by creating a slope at the mesa edge, is proposed and verified to completely suppress the formation of dark line defects. By comparing the experimental observations of dark line defects formation with the maximum shear stress present for different slopes of the mesa wall, the boundaries were determined for initiating dislocation slip.

AlGaN-based UVC LD structures were grown on single-crystal AlN substrates by metal organic vapor phase epitaxy. Each UV-C LD consists of a 350-nm-thick n-type $Al_{0.7}Ga_{0.3}N$ n-clad layer, a 100-nm-thick $Al_{0.63}Ga_{0.37}N$ waveguide layer with multiple quantum wells, a 320-nm-thick p-type distributed-polarization doped (p-DPD) cladding layer with an average Al composition of 0.85, and a p-contact layer. Details of the UV-C LD structure and fabrication procedure can be found in a previous report[2]. A dry etching process us-

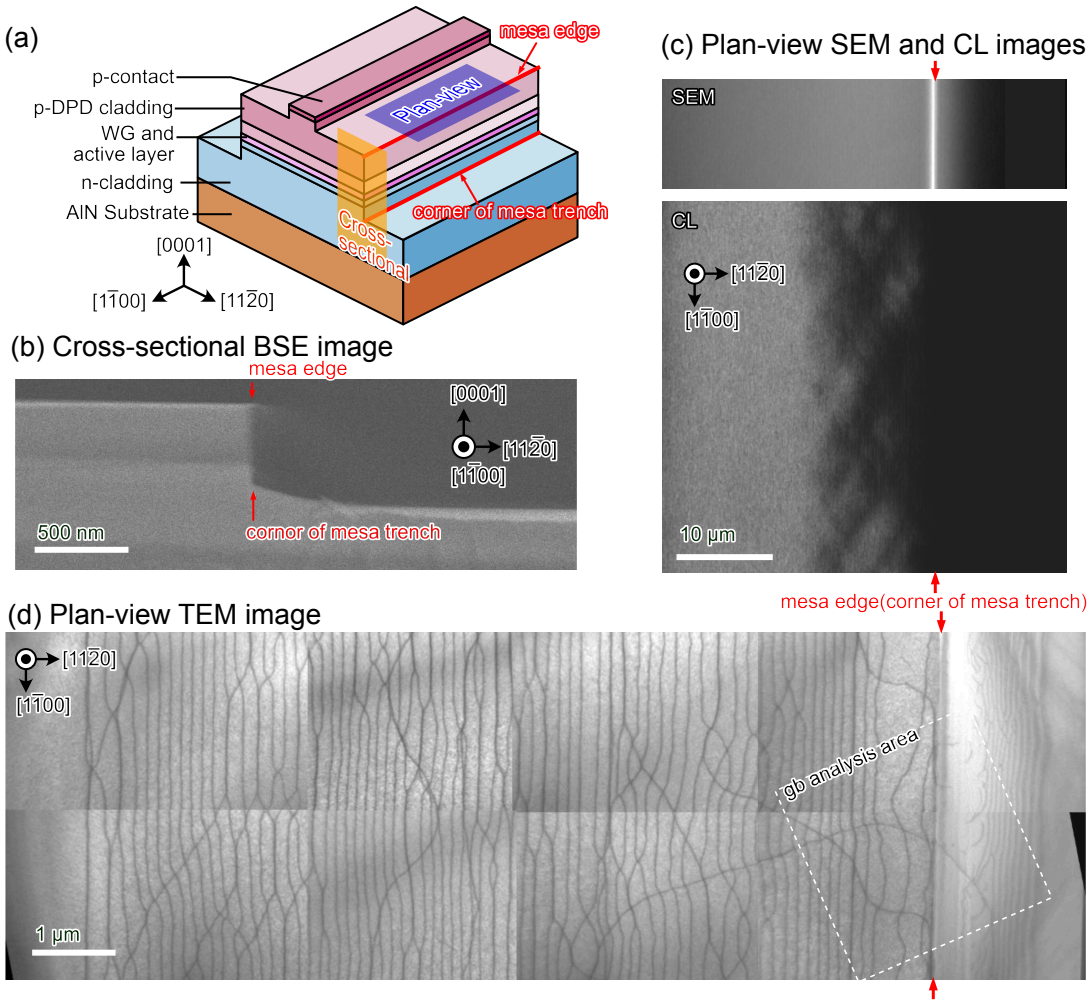

FIG. 1. Analysis of dark line defects appearing at mesa edge. (a) Schematic of the UV-C LD mesa structure. (b) Cross-sectional BSE image. (c) Plan-view SEM and CL images. (d) Plan-view TEM image.

ing Cl gas was employed to isolate the p-contact layer for current narrowing while simultaneously forming the mesa stripes along the $[1\bar{1}00]$ direction. Electrode metal deposition (used in the standard LD fabrication process) was not carried out to enable further analysis, while thermal treatments, i.e. the rapid thermal annealing of 850 °C for n-metal and that of 550 °C for p-metal, were performed just as in the actual electrode fabrication process. A schematic drawing of the fabricated structure is shown in Fig. 1(a).

The fabricated structure was observed by cross-sectional backscattered electron microscopy (BSE), plan-view cathodoluminescence (CL), and plan-view scanning electron microscopy (SEM) and transmission electron microscopy (TEM). The schematic of the viewing spots and orientations is depicted in Fig. 1(a). As shown in Fig. 1(b), the conventional mesa trench is etched down to the n-cladding layer, and the mesa angle is nearly perpendicular to the epilayer surface. For the plan-view CL measurement, monochromatic imaging was used to observe the emission of the active layer. Dark line defects, where radiative recombination was inhibited, were observed as far as 12 μm inside the mesa edge. As shown in the planar TEM image in Fig. 1(d), numerous dislocation lines were observed within the region where dark line defects appeared in the CL image. No dislocation lines could be found more than 12 μm away from the the mesa edge. Therefore, it is clear that dislocation generation induces the formation of nonemitting regions. The observed dislocation lines are mostly in $[1\bar{1}00]$ direction while some extending diagonally. Those dislocations running parallel to the $[1\bar{1}00]$ direction appear to be part of dislocation loops which start at the mesa wall. In fact, there are small half-loop defects near the corner of the mesa trench on the etched surface. The dislocations further from the mesa edge become more parallel to the mesa stripe. This seems likely to be due to the repulsive interaction of small dislocation loops with identical Burgers vectors[7].

To determine the Burgers vectors of the observed dislocations, $g \cdot b$ analysis was carried out for the designated area at the mesa edge, as shown in Fig. 1(d). Figure 2 shows the plan-view TEM images observed under the $[0001]$ zone axis and $g = \bar{1}100$, $g = 01\bar{1}0$, and $g = 11\bar{2}0$ conditions. The contrast vanished for all dislocations observed under the $g = \bar{1}100$ condition compared with other observed dislocations, indicating

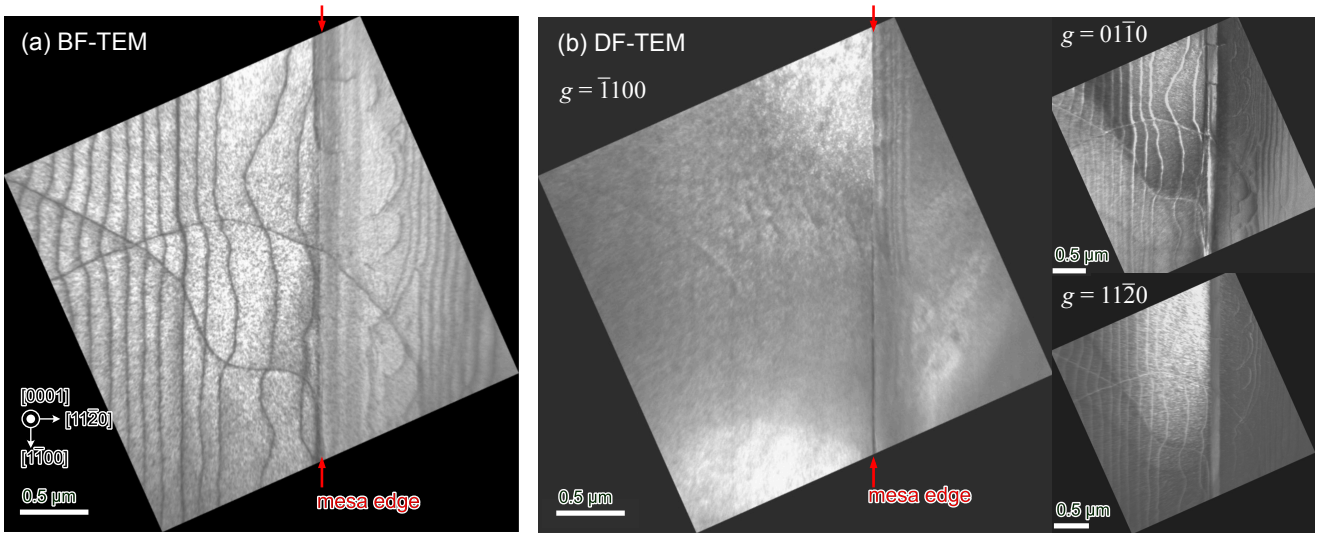

FIG. 2. Plan-view TEM images at the the mesa edge under (a) Bright-field image with $[0001]$ zone axis and (b) dark field images with $g = \bar{1}100$, $g = 1\bar{1}00$, and $g = 11\bar{2}0$.

that the Burgers vector of the observed dislocations is parallel to the $[11\bar{2}0]$ direction which corresponds to $g \cdot b = 0$. This result showed dislocation lines in the direction of $[1\bar{1}00]$ consistent with (0001) basal plane slip, $\{0001\}\langle 11\bar{2}0\rangle$[12,13]. No partial dislocations or stacking faults were found providing strong evidence that the observed dislocations were the result of slip due to forces perpendicular to the mesa stripe.

The occurrence of basal plane slip at mesa structures has been reported in other material systems such as InGaN/GaN and AlN/SiC heterostructures[7,14,15]. One feature in common with our study is that the epitaxial layers are being grown with large strains due to lattice mismatch, and the symmetry of the plane stress is broken by the formation of mesa trench. The mesa wall will elastically deform after mesa formation, because the walls of the mesa are no longer constrained and strain will be relieved. In the aforementioned studies, the unconstrained endpoints of heterointerfaces at the mesa wall become spots where high shear stresses concentrate. Consequently, the dislocations are propagated from the mesa wall along the heterointerfaces in proportion to shear stress that increases with the strain of epitaxial layer. In the case of the InGaN/GaN mesa structure, for instance, dislocation loops were formed when the misfit strain was greater than 2.3%, and the dislocation penetration depth becomes larger as the misfit strain increases as a result of an increase in the indium composition.[7] Another common feature is a relatively low density of threading dislocations so that the glide of dislocations along the basal plane is not overly suppressed by entanglement with the threading dislocations. The most significant difference from previous studies is that the mesa trench is etched down to the n-cladding layer which is subjected to compressive stress of about 3 GPa by pseudomorphic growth on the AlN substrate. Therefore, the corners of the mesa trench, which are etched into the highly strained n-cladding layer, can also become spots where shear stresses are concentrated. Indeed, the observed dislocations were not at any of the heterointerfaces in the LD structure, but rather were observed in the uniform n-AlGaN cladding layer where they appear to have glided in from the corners of the mesa trench. Since the shape of the mesa will change the shear stress distribution at the corners of the mesa trench, an appropriate control of the mesa wall might enable the control of the formation of dislocations[16]. Also, the dislocations are formed not after epitaxial growth but only after heat treatment of the etched mesa at high temperature[3]. On the basis of discussions above, the relationship between the shape of the mesa and the shear stress distribution, as well as the effect of annealing were quantitatively investigated.

TABLE I. Lattice constants and elastic constants (in GPa unit) used in the simulation. Values for $Al_xGa_{1-x}N$ were interpolated using Vegard's law.

	a (nm)	C_{11}	C_{12}	C_{13}	C_{33}	C_{44}
GaN[a]	0.3186	373	141	80	387	94
AlN[b]	0.3112	394	134	95	402	121

[a] Reference[17]
[b] Reference[18]

The residual shear stress was numerically simulated by the finite element method (FEM) to gain insight into its distribution and magnitude as a function of the mesa shape. Both AlGaN and AlN were modeled as anisotropic elastic materials. The Cartesian coordinates x, y, and z stand for the crystallographic directions of $[11\bar{2}0]$, $[1\bar{1}00]$, and $[0001]$, respectively. The elastic constants of AlGaN in the 6×6 elastic matrix with six fold symmetry were defined using Vegard's law considering the constants listed in Table I. The p-DPD cladding layer was modeled as a single layer of $Al_{0.85}Ga_{0.15}N$ with an average Al composition.

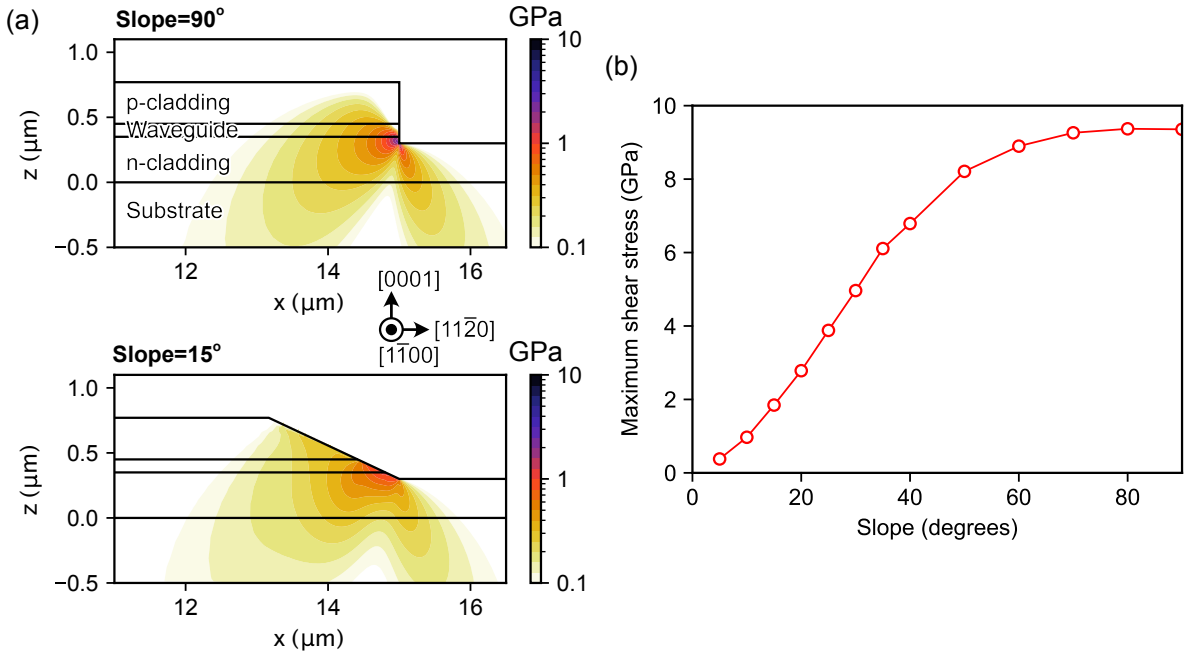

FIG. 3. (a) Distribution of shear stress σ_{zx} at the corner of mesa trench for a vertical mesa and a mesa with a 15° slope to the surface. (b) The maximum shear stress at the mesa edge is plotted as a function of slope (measured in degrees from the surface).

The simulated layer model is based on the structure after the actual process, wherein the p-contact layer was removed and the mesa trench depth was over-etched into the n-cladding layer by 50 nm. The back of the substrate (whose thickness is set to 5 μm in the model) is considered to be fixed boundary. Other surfaces of the structure are considered to be free boundaries. An initial compressive strain of

$$\varepsilon_{xx} = \varepsilon_{yy} = -\frac{a_{\mathrm{AlGaN}} - a_{\mathrm{AlN}}}{a_{\mathrm{AlGaN}}}$$

corresponding to pseudomorphic growth on the AlN substrate, is applied to each layer. The commercial COMSOL multiphysics FEM solver package was used to obtain numerical solutions to the cross-sectional strain and stress distributions at the corner of mesa trench. Figure 3(a) shows the calculated shear stresses σ_{zx} for two examples of mesa shapes. The first simulation is for a vertical mesa structure which is similar to the fabrication result described above. A considerable concentration of shear stress is observed at the corner of mesa trench with a maximum value of more than 9 GPa. Note that while a negative range of shear stress distribution exists in the p-clad layer and interface with the waveguide, this distribution is not shown here since its magnitude is more than one order smaller than the positive stresses. For the 15°-sloped mesa shown in Fig. 3(a), the maximum shear stress was reduced to less than 1 GPa. Figure 3(b) shows the maximum shear stress calculated for the corner of mesa trench for various degrees of the slope. The simulation results show that reducing the mesa-slope angle to less than 50° is effective in reducing the shear stress concentration at the corner of mesa trench.

The Vickers hardnesses for single-crystal GaN and AlN at room temperature are reported to be 10 GPa and 17 GPa, respectively[19]. Although there are no reported hardness at the AlGaN concentrations used in the current devices, they are expected to be in this range. As shown in Fig. 3(b), the maximum shear stress never falls within this range and, therefore, plastic deformation is unlikely to occur even for a vertical mesa structure. Indeed, no dark line defects are observed in the CL image before heat treatment.[3] However, the Vickers hardness decreases with increasing temperature, reaching 3.5 GPa and 6 GPa at 600 °C for GaN and AlN, respectively,[19] which is the threshold temperature at which dark line defects appeared at the mesa stripe. The maximum shear stress associated with a vertical slope likely exceeds this Vickers hardness range at 600 °C. Considering that the Peierls stress, which describes the minimum shear stress necessary for a dislocation to glide along the {0001} shuffle slip plane[20], is calculated to be 3-4 GPa for both AlN and GaN[21–23] and that threading dislocations, which can inhibit glide through entanglement, are absent in the current AlGaN/AlN system, it is expected that once the criteria for plastic deformation are reached, the distribution of dislocations toward the inside of the mesa stripe, as described in the experimental observations, will easily occur. It also appears that by forming mesa with a slope less than 20°, plastic deformation during thermal annealing (which is required for electrode formation) can be avoided since this small slope would keep the maximum shear stress less than 3 GPa.

Armed with the insights gained from the FEM simulations, the LD mesa stripe with sloped edges was fabricated. A cross-sectional BSE image is shown in Fig. 4(a). The

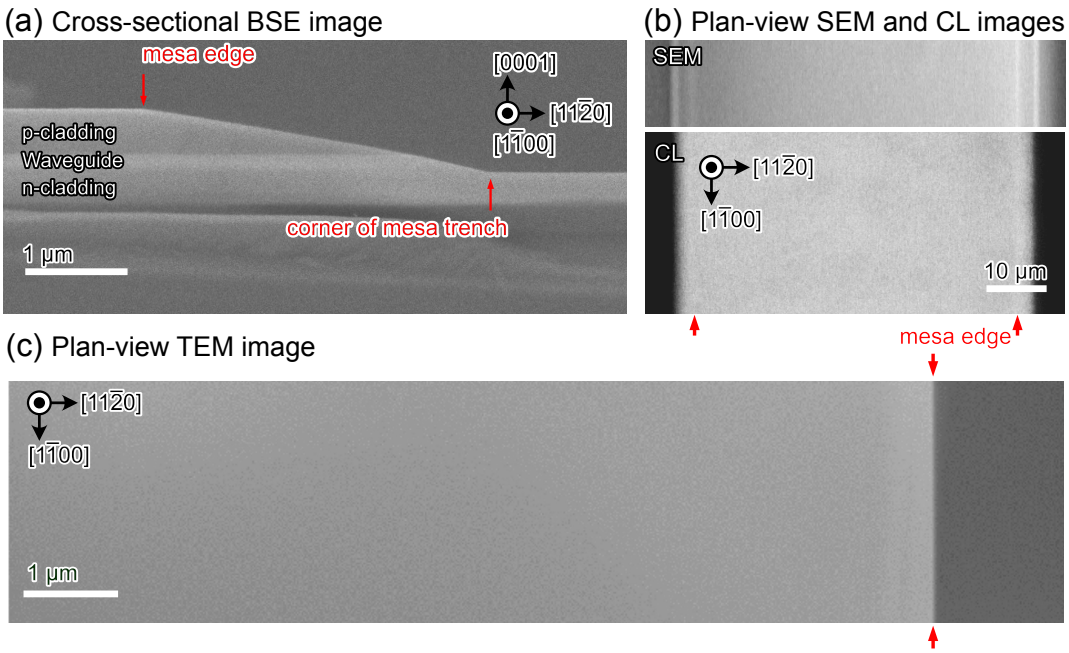

FIG. 4. (a) Cross-sectional BSE image of fabricated sloped mesa structure. (b) Plan-view SEM and CL images. (c) Plan-view TEM image.

sloped mesa was formed by conventional dry etching with a varied-thickness etching mask by thermal reflow of the photoresist[24,25]. A fabricated slope inclination of 15° to the surface was obtained with good reproducibility. Plan-view SEM, CL, and TEM imaging were carried out and results are shown in Fig. 4(b) and (c). Clearly, no dislocation-induced dark line defects are observed at the mesa stripe using with slope structure, and uniform CL emission is observed across the entire mesa stripe.

The present results emphasize the importance of managing the mesa-shape-induced residual shear stress in highly strained pseudomorphic nitride structures. Although the use of pseudomorphic AlGaN is highly successful in reducing the dislocation density in the device layers by inhibiting the formation of misfit dislocations, it also leaves the device layers highly strained. As described in the present paper shows, device processing can then easily result in very high shear stresses when mesas are etched into the structure. These high shear stresses can then result in dislocations being pushed into the active region of the device, causing the degradation of performance and the likelihood of reduced reliability.[26] However, the present study reveals that the fabrication structures can be engineered to optimize both performance and reliability with respect to dislocation motion, even with these highly strained structures. For AlGaN based UV-C LDs, this technique has been used to reduce restrictions on electrode design to avoid current flow through regions of high dislocation densities near the mesa edges and to reduce the series resistance of the device, resulting in substantial benefits. The improved understanding of dislocation formation may eventually enable further reductions in the series resistance by increasing the side-wall slope to further reduce the distance electrons need to travel for current injection.

In this study, a detailed analysis revealed that the dark-line defects appearing at the edge of the mesa of UV-C LDs may be attributed to basal plane dislocations which result from the localization of shear stresses associated with mesa formation in a highly strained layers. Controlling the local shear stress by means of a tilted mesa structure was verified by modeling and experiments have proven it to be a practical method of effectively suppressing dislocation generation. The considerations and technique proposed here not only provided a critical breakthrough in reducing the device resistance of UV-C LDs, but also are expected to improve the performance of optoelectrical devices using pseudomorphic AlGaN/AlN systems.

ACKNOWLEDGMENTS

The authors would like to thank Professor Nobuyuki Ikarashi of Nagoya University and Dr. Masato Toita, Mr. Kazuhiro Nagase, and Dr. Naohiro Kuze of Asahi Kasei Corporation for invaluable discussion and considerable support. The authors would like to acknowledge the support of the Center for Integrated Research of Future Electronics, Transformative Electronics Facilities (C-TEFs) of Nagoya University for the use of their facilities for device fabrication. This work was supported by JSPS KAKENHI Grant Number 21H04560.

[1]Z. Zhang, M. Kushimoto, T. Sakai, N. Sugiyama, L. J. Schowalter, C. Sasaoka, and H. Amano, "A 271.8 nm deep-ultraviolet laser diode for room temperature operation," Applied Physics Express **12**, 124003 (2019).
[2]Z. Zhang, M. Kushimoto, A. Yoshikawa, K. Aoto, L. J. Schowalter, C. Sasaoka, and H. Amano, "Continuous-wave lasing of AlGaN-based ultraviolet laser diode at 274.8 nm by current injection," Applied Physics Express **15**, 041007 (2022).

[3]M. Kushimoto, Z. Zhang, N. Sugiyama, Y. Honda, L. J. Schowalter, C. Sasaoka, and H. Amano, "Impact of heat treatment process on threshold current density in AlGaN-based deep-ultraviolet laser diodes on AlN substrate," Applied Physics Express **14**, 051003 (2021).

[4]J. Grandusky, J. Smart, M. Mendrick, L. Schowalter, K. Chen, and E. Schubert, "Pseudomorphic growth of thick n-type AlxGa1-xN layers on low-defect-density bulk AlN substrates for UV LED applications," Journal of Crystal Growth **311**, 2864–2866 (2009).

[5]J. R. Grandusky, S. R. Gibb, M. C. Mendrick, and L. J. Schowalter, "Properties of Mid-Ultraviolet Light Emitting Diodes Fabricated from Pseudomorphic Layers on Bulk Aluminum Nitride Substrates," Applied Physics Express **3**, 072103 (2010).

[6]Z. Zhang, M. Kushimoto, T. Sakai, N. Sugiyama, L. J. Schowalter, C. Sasaoka, and H. Amano, "Design and characterization of a low-optical-loss UV-C laser diode," Japanese Journal of Applied Physics **59**, 094001 (2020).

[7]J. Mei, R. Liu, F. A. Ponce, H. Omiya, and T. Mukai, "Basal-plane slip in InGaN/GaN heterostructures in the presence of threading dislocations," Applied Physics Letters **90**, 171922 (2007).

[8]P. G. Neudeck, H. Du, M. Skowronski, D. J. Spry, and A. J. Trunek, "Growth and characterization of 3C–SiC and 2H–AlN/GaN films and devices produced on step-free 4H–SiC mesa substrates," Journal of Physics D: Applied Physics **40**, 6139–6149 (2007).

[9]R. Liu, J. Mei, S. Srinivasan, F. A. Ponce, H. Omiya, Y. Narukawa, and T. Mukai, "Generation of misfit dislocations by basal-plane slip in InGaN/GaN heterostructures," Applied Physics Letters **89**, 201911 (2006).

[10]J.-L. Gosselin and P. Valizadeh, "Theoretical Evaluation of the Effects of Isolation-Feature Size and Geometry on the Built-In Strain and 2-D Electron Gas Density of AlGaN/GaN Heterostructures," IEEE Transactions on Electron Devices **65**, 4800–4806 (2018).

[11]Y. Kawakami, A. Kaneta, L. Su, Y. Zhu, K. Okamoto, M. Funato, A. Kikuchi, and K. Kishino, "Optical properties of InGaN/GaN nanopillars fabricated by postgrowth chemically assisted ion beam etching," Journal of Applied Physics **107**, 023522 (2010).

[12]K. A. Jones and I. G. Batyrev, "The structure of dislocations in (In,Al,Ga)N wurtzite films grown epitaxially on (0001) or (11$\bar{2}$2) GaN or AlN substrates," Journal of Applied Physics **112**, 113507 (2012).

[13]V. Audurier, J. L. Demenet, and J. Rabier, "AIN plastic deformation between room temperature and 800°C. I. Dislocation substructure observations," Philosophical Magazine A **77**, 825–842 (1998).

[14]M. E. Twigg, N. D. Bassim, M. A. Mastro, C. R. Eddy, R. L. Henry, J. C. Culbertson, R. T. Holm, P. Neudeck, J. A. Powell, and A. J. Trunek, "Strain relief and dislocation motion in III-nitride films grown on stepped and step-free 4H-SiC mesas," Journal of Applied Physics **101**, 053509 (2007).

[15]N. Bassim, M. Twigg, M. Mastro, C. Eddy, T. Zega, R. Henry, J. Culbertson, R. Holm, P. Neudeck, J. Powell, and A. Trunek, "Dislocations in III-nitride films grown on 4H-SiC mesas with and without surface steps," Journal of Crystal Growth **304**, 103–107 (2007).

[16]Y. Takada, J. Osaka, Y. Ishikawa, and K. Wada, "Effect of Mesa Shape on Threading Dislocation Density in Ge Epitaxial Layers on Si after Post-Growth Annealing," Japanese Journal of Applied Physics **49**, 04DG23 (2010).

[17]M. Yamaguchi, T. Yagi, T. Sota, T. Deguchi, K. Shimada, and S. Nakamura, "Brillouin scattering study of bulk GaN," Journal of Applied Physics **85**, 8502–8504 (1999).

[18]M. Kazan, E. Moussaed, R. Nader, and P. Masri, "Elastic constants of aluminum nitride," physica status solidi (c) **4**, 204–207 (2007).

[19]I. Yonenaga, "High-temperature strength of III V nitride crystals," Journal of Physics: Condensed Matter **14**, 12947–12951 (2002).

[20]I. Belabbas, J. Chen, and G. Nouet, "Energetics and core structure of the undissociated basal screw dislocation in wurtzite GaN," physica status solidi c **13**, 221–224 (2016).

[21]Y. Tokumoto, K. Kutsukake, Y. Ohno, and I. Yonenaga, "Dislocation structure in AlN films induced by *in situ* transmission electron microscope nanoindentation," Journal of Applied Physics **112**, 093526 (2012).

[22]M. Fujikane, T. Yokogawa, S. Nagao, and R. Nowak, "Yield shear stress dependence on nanoindentation strain rate in bulk GaN crystal," physica status solidi c **8**, 429–431 (2011).

[23]P. G. Caldas, E. M. Silva, R. Prioli, J. Y. Huang, R. Juday, A. M. Fischer, and F. A. Ponce, "Plasticity and optical properties of GaN under highly localized nanoindentation stress fields," Journal of Applied Physics **121**, 125105 (2017).

[24]F. Yan, C. Qin, J. H. Zhao, and M. Weiner, "A Novel Technology for the Formation of a Very Small Bevel Angle for Edge Termination," Materials Science Forum **389–393**, 1305–1308 (2002).

[25]T. Maeda, T. Narita, H. Ueda, M. Kanechika, T. Uesugi, T. Kachi, T. Kimoto, M. Horita, and J. Suda, "Design and Fabrication of GaN p-n Junction Diodes With Negative Beveled-Mesa Termination," IEEE Electron Device Letters **40**, 941–944 (2019).

[26]S. Tomiya, H. Nakajima, K. Funato, T. Miyajima, K. Kobayashi, T. Hino, S. Kijima, T. Asano, and M. Ikeda, "Dislocations in GaN-Based Laser Diodes on Epitaxial Lateral Overgrown GaN Layers," physica status solidi (a) **188**, 69–72 (2001).